Influence of Doppler broadening and spontaneously generated coherence on propagation effect in a quasi lambda-type four-level system*

Liu Zhong-Bo(刘中波), Liang Ying(梁 颖),
Jia Ke-Ning(贾克宁), and Fan Xi-Jun(樊锡君)†

College of Physics and Electronics, Shandong Normal University, Jinan 250014, *China*

(Received 5 August 2010; revised manuscript received 4 September 2011)

In this paper we study influences of Doppler broadening, spontaneously generated coherence, and other system parameters on propagation effect in a quasi lambda-type four-level atomic system. It is shown that when the Doppler broadening is present, generally speaking, the values of gain and intensity of lasing without inversion (i.e. the probe field) in the co-propagating probe and driving fields case are much larger than those in the counter-propagating case; considerably larger gain and intensity of lasing without inversion than those without the Doppler broadening can be obtained by choosing appropriate values of the Doppler broadening width and spontaneously generated coherence strength. The gain and intensity of lasing without inversion increase with the increase of spontaneously generated coherence strength; when spontaneously generated coherence is present, much larger gain and intensity of lasing without inversion than those in the case without spontaneously generated coherence can be obtained. Choosing suitable values of the probe detuning, Rabi frequencies of the driving and pump fields at the entrance of the medium also can remarkably enhance the gain and intensity of lasing without inversion.

Keywords: four-level system, propagation effect, spontaneously generated coherence, Doppler broadening, lasing without inversion

PACS: 42.50.Gy, 42.50.Nn **DOI:** 10.1088/1674-1056/21/2/024206

1. Introduction

A kind of coherence can be created by interference of spontaneous emission, usually called as spontaneously generated coherence (SGC). In the last few decades there has been intensive interest in the study of SGC.[1−25] The study shows that SGC is responsible for many important physical phenomena, such as lasing without inversion (LWI),[26] electromagnetically induced transparency (EIT),[27−29] coherent population trapping (CPT),[30] high dispersion with zero absorption,[31] quantum information and computation,[32] etc. In these physical phenomena, LWI has attracted much more attention,[33−35] since the study for LWI has an important scientific sense and potential for wide applications. The investigations into the effects of SGC are mostly related to three-level atomic systems, there are only a few papers considering more complex atomic system — four-level atomic system[8,9,21,23,25] and these papers used the static atomic systems. In fact, many pieces of experimental research on optical phenomena, such as LWI, usually use an atomic vapour, in which Doppler broadening is very significant. The results of study show that, the Doppler broadening has a great influence on LWI gain in an atomic system without SGC.[36−42] In addition, the propagation effect also can considerably affect the LWI gain. So far, all investigations about propagation effect only considered different typical three-level atomic systems.[43−46] One of the most important goals in the study for LWI is to obtain larger LWI gain and intensity. In this paper, we explore theoretically the influences of SGC, Doppler broadening and other parameters on propagation effect in a four-level atomic system and find a way to obtain larger LWI gain and intensity. To our best knowledge, so far there is not such a study.

2. System model and equations of motion

The quasi lambda (Λ)-type four-level atomic system considered here is shown in Fig. 1. The transition

*Project supported by the National Natural Science Foundation of China (Grant No. 10875072).
†Corresponding author. E-mail: xjfan108@yahoo.com.cn
© 2012 Chinese Physical Society and IOP Publishing Ltd

$|2\rangle \rightarrow |3\rangle$ with frequency ω_{23} is coupled by a strong driving field of frequency $\omega_{\rm c}$ with Rabi frequency $\Omega_{\rm c} = \boldsymbol{\mu}_{32} \cdot \boldsymbol{E}_{\rm c}/(2\hbar)$ while the transition $|1\rangle \rightarrow |3\rangle$ with frequency ω_{13} is coupled by a weak probe field of frequency $\omega_{\rm p}$ with Rabi frequency $\Omega_{\rm p} = \boldsymbol{\mu}_{31} \cdot \boldsymbol{E}_{\rm p}/(2\hbar)$. A coherent pump field of frequency $\omega_{\rm s}$ with Rabi frequency $\Omega_{\rm s} = \boldsymbol{\mu}_{41} \cdot \boldsymbol{E}_{\rm s}/(2\hbar)$ is applied between levels $|1\rangle$ and $|4\rangle$.

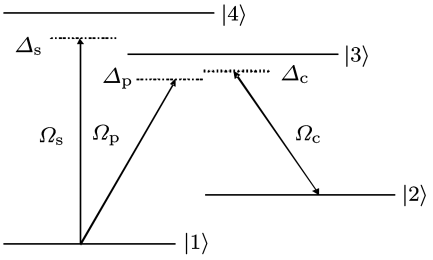


Fig. 1. Quasi Λ-type four-level system.

Using the rotating-wave and electric dipole approximations, we can write the density matrix equations of motion of this system with SGC as[9]

$$\dot{\rho}_{11} = \gamma_{31}\rho_{33} + \gamma_{41}\rho_{44} + {\rm i}\Omega_{\rm p}^{*}\rho_{31} - {\rm i}\Omega_{\rm p}\rho_{13} + {\rm i}\Omega_{\rm s}^{*}\rho_{41} - {\rm i}\Omega_{\rm s}\rho_{14}, \tag{1a}$$

$$\dot{\rho}_{22} = \gamma_{32}\rho_{33} + \gamma_{42}\rho_{44} + {\rm i}\Omega_{\rm c}^{*}\rho_{32} - {\rm i}\Omega_{\rm c}\rho_{23}, \tag{1b}$$

$$\dot{\rho}_{33} = -(\gamma_{31} + \gamma_{32})\rho_{33} + {\rm i}\Omega_{\rm p}\rho_{13} - {\rm i}\Omega_{\rm p}^{*}\rho_{31} + {\rm i}\Omega_{\rm c}\rho_{23} - {\rm i}\Omega_{\rm c}^{*}\rho_{32}, \tag{1c}$$

$$\dot{\rho}_{44} = -(\gamma_{41} + \gamma_{42})\rho_{44} + {\rm i}\Omega_{\rm s}\rho_{14} - {\rm i}\Omega_{\rm s}^{*}\rho_{41}, \tag{1d}$$

$$\dot{\rho}_{12} = {\rm i}(\Delta_{\rm p} - \Delta_{\rm c})\rho_{12} + {\rm i}\Omega_{\rm p}^{*}\rho_{32} + {\rm i}\Omega_{\rm s}^{*}\rho_{42} - {\rm i}\Omega_{\rm c}\rho_{13} + \sqrt{\gamma_{31}\gamma_{32}}p_1\rho_{33} + \sqrt{\gamma_{41}\gamma_{432}}p_2\rho_{44}, \tag{1e}$$

$$\dot{\rho}_{13} = -[(\gamma_{31} + \gamma_{32})/2 - {\rm i}\Delta_{\rm p}]\rho_{13} + {\rm i}\Omega_{\rm s}^{*}\rho_{43} - {\rm i}\Omega_{\rm c}^{*}\rho_{12} + {\rm i}\Omega_{\rm p}^{*}(\rho_{33} - \rho_{11}), \tag{1f}$$

$$\dot{\rho}_{14} = -[(\gamma_{41} + \gamma_{42})/2 - {\rm i}\Delta_{\rm s}]\rho_{14} + {\rm i}\Omega_{\rm p}^{*}\rho_{34} + {\rm i}\Omega_{\rm s}^{*}(\rho_{44} - \rho_{11}), \tag{1g}$$

$$\dot{\rho}_{23} = -[(\gamma_{31} + \gamma_{32})/2 - {\rm i}\Delta_{\rm c}]\rho_{23} - {\rm i}\Omega_{\rm p}^{*}\rho_{21} + {\rm i}\Omega_{\rm c}^{*}(\rho_{33} - \rho_{22}), \tag{1h}$$

$$\dot{\rho}_{24} = -[(\gamma_{41} + \gamma_{42})/2 - {\rm i}(\Delta_{\rm s} - \Delta_{\rm p} + \Delta_{\rm c})]\rho_{24} + {\rm i}\Omega_{\rm c}^{*}\rho_{34} - {\rm i}\Omega_{\rm s}^{*}\rho_{21}, \tag{1i}$$

$$\dot{\rho}_{34} = -[(\gamma_{31} + \gamma_{32} + \gamma_{41} + \gamma_{42})/2 - {\rm i}(\Delta_{\rm s} - \Delta_{\rm p})]\rho_{34} + {\rm i}\Omega_{\rm p}\rho_{14} + {\rm i}\Omega_{\rm c}\rho_{24} - {\rm i}\Omega_{\rm s}^{*}\rho_{31}. \tag{1j}$$

The above equations are constrained by $\rho_{mn}^{*} = \rho_{nm}$ and $\rho_{11} + \rho_{22} + \rho_{33} + \rho_{44} = 1$. Here ρ_{mm} is the atomic population of state $|m\rangle$, and ρ_{mn} $(m \neq n)$ is the atomic polarization between states $|m\rangle$ and $|n\rangle$; γ_{mn} represents the spontaneous decay rate from level $|m\rangle$ to $|n\rangle$, in Eqs. (1) we neglected the spontaneous decay rate γ_{21} from level $|2\rangle$ to $|1\rangle$; $\Delta_{\rm s}(= \omega_{41} - \omega_{\rm s})$, $\Delta_{\rm p}(= \omega_{31} - \omega_{\rm p})$, and $\Delta_{\rm c}(= \omega_{32} - \omega_{\rm p})$ denote the frequency detuning of the pump, probe and driving fields from their relevant atomic transitions, respectively. The $\sqrt{\gamma_{31}\gamma_{32}}p_1\rho_{33}$ and $\sqrt{\gamma_{41}\gamma_{42}}p_2\rho_{44}$ represent the quantum interference effect from the cross-coupling, i.e. SGC effect. The parameter p_1 is defined as $p_1 \equiv \boldsymbol{\mu}_{31} \cdot \boldsymbol{\mu}_{32}/|\boldsymbol{\mu}_{31}||\boldsymbol{\mu}_{32}| = \cos(\theta_1)$, and θ_1 represents the angle between the two dipole moments $\boldsymbol{\mu}_{31}$ and $\boldsymbol{\mu}_{32}$; $p_2 \equiv \boldsymbol{\mu}_{41} \cdot \boldsymbol{\mu}_{42}/|\boldsymbol{\mu}_{41}||\boldsymbol{\mu}_{42}|$, and θ_2 represents the angle between the two dipole moments $\boldsymbol{\mu}_{41}$ and $\boldsymbol{\mu}_{42}$. If $\boldsymbol{\mu}_{31}$ and $\boldsymbol{\mu}_{32}$ ($\boldsymbol{\mu}_{41}$ and $\boldsymbol{\mu}_{42}$) are orthogonal to each other, then $\theta_1 = \pi/2$ ($\theta_2 = \pi/2$), p_1 (p_2) $= 0$ and SGC is absent; otherwise $\theta_1 \neq \pi/2$ ($\theta_2 \neq \pi/2$), then p_1 (p_2) $\neq 0$ and the SGC is present. The strength of the SGC effect will vary with the varying values of θ_1 and θ_2. If level $|4\rangle$ is absent, equations (1) reduce to the equations of motion for a Λ-type three-level atomic system with SGC,[7] so the system which we are considering is called as a quasi Λ-type four-level atomic system.

Using the slowly varying envelope and the rotating-wave approximations, we can write the propagation equations of the probe, driving and pump fields as

$$\frac{\partial}{\partial z}\Omega_{\rm p}(z) = \frac{3N\gamma_{31}\lambda_{\rm p}^{2}}{8\pi}{\rm Im}\,\rho_{13}(z), \tag{2a}$$

$$\frac{\partial}{\partial z}\Omega_{\rm c}(z) = \frac{3N\gamma_{32}\lambda_{\rm c}^{2}}{8\pi}{\rm Im}\,\rho_{23}(z), \tag{2b}$$

$$\frac{\partial}{\partial z}\Omega_{\rm s}(z) = \frac{3N\gamma_{41}\lambda_{\rm s}^{2}}{8\pi}{\rm Im}\,\rho_{14}(z), \tag{2c}$$

where, N is the atom density, $\lambda_{\rm p}$, $\lambda_{\rm c}$, and $\lambda_{\rm s}$ represent the probe, driving, and pump wavelengths respectively.

Up to now, the above discussion has referred to the static atomic systems without Doppler broadening. In order to account for the Doppler broadening one should consider, in Eqs. (1), the velocity-dependent detunings given by

$$\Delta_{\rm p}(v) = \Delta_{\rm p}^{0} \pm \omega_{\rm p}v/c, \tag{3a}$$

$$\Delta_{\rm c}(v) = \Delta_{\rm c}^{0} \pm \omega_{\rm c}v/c, \tag{3b}$$

$$\Delta_{\rm s}(v) = \Delta_{\rm s}^{0} \pm \omega_{\rm s}v/c, \tag{3c}$$

where, v is the velocity of single atom moving along z axis, c is the light speed, $\Delta_{\rm p}^{0} \equiv \Delta_{\rm p}(v = 0) = \omega_{31} - \omega_{\rm p}$, $\Delta_{\rm c}^{0} \equiv \Delta_{\rm c}(v = 0) = \omega_{32} - \omega_{\rm c}$, and $\Delta_{\rm s}^{0} \equiv \Delta_{\rm s}(v = 0) = \omega_{41} - \omega_{\rm s}$ are the detunings of the probe, driving and pump fields, respectively, when the atom is static

($\upsilon = 0$), the negative (positive) sign corresponds to co-propagating (counter-propagating) atom and field. For convenience, in the following calculations we assume that the driving and pump fields all propagate in the direction along which the atoms move, so co-propagating (counter-propagating) probe and driving fields mean co-propagating (counter-propagating) probe field and atom. Under this condition, we only need to take the negative signs in Eqs. (3b) and (3c).

We assume that atomic velocity obeys Maxwell distribution:

$$N(\upsilon) = \frac{N_0}{\sigma\sqrt{\pi}} \exp\left(-\frac{\upsilon^2}{\sigma^2}\right), \tag{4}$$

where σ represents the most probable velocity and the width of the Doppler broadening induced by emission transition at the half-maximum position is

$$D = 2\sqrt{\ln 2}\frac{\sigma}{c}\omega_{\rm p}. \tag{5}$$

Considering the effect of the Doppler broadening, we need to write the propagation equations of the probe, driving, and pump fields as:

$$\frac{\partial}{\partial z}\Omega_{\rm p}(z) = \frac{3\gamma_{31}\lambda_{\rm p}^2}{8\pi}\int N(\upsilon){\rm Im}\,\rho_{13}(z,\upsilon)\,{\rm d}\upsilon, \tag{6a}$$

$$\frac{\partial}{\partial z}\Omega_{\rm c}(z) = \frac{3\gamma_{32}\lambda_{\rm c}^2}{8\pi}\int N(\upsilon){\rm Im}\,\rho_{23}(z,\upsilon)\,{\rm d}\upsilon, \tag{6b}$$

$$\frac{\partial}{\partial z}\Omega_{\rm s}(z) = \frac{3\gamma_{41}\lambda_{\rm s}^2}{8\pi}\int N(\upsilon){\rm Im}\,\rho_{14}(z,\upsilon)\,{\rm d}\upsilon. \tag{6c}$$

The probe gain (absorption) coefficient corresponds to the imaginary part of ρ_{13}. If ${\rm Im}\,\rho_{13} > 0$, the system exhibits gain for the probe field; if ${\rm Im}\,\rho_{13} < 0$, the probe field is attenuated. When $\rho_{11} > \rho_{33}$ and ${\rm Im}\,\rho_{31} > 0$ are simultaneously satisfied, LWI gain can be obtained, then LWI can be realized. The probe field is the LWI field.

3. Numerical results and discussion

In the following, we shall analyse the influence of SGC on the propagation effect in a Doppler broadened quasi Λ-type four-level atomic system for both cases without and with the Doppler broadening by using the numerical results from Eqs. (1), (2), and (6). Except for special statement, the system parameters take the following values: $N_0 = 2\times10^{15}$ atoms/m^3; $\lambda_{\rm p} = 794.9703$ nm, $\lambda_{\rm c} = 794.9843$ nm, $\lambda_{\rm s} = 794.9686$ nm; $\gamma_{31} = 2\pi\times 6$ MHz, $\gamma_{32} = \gamma_{31}$, $\gamma_{41} = \gamma_{42} = 1.2\gamma_{31}$; $\Delta_{\rm p}^0 = 4.9\gamma_{31}$, $\Delta_{\rm c}^0 = 0$, and $\Delta_{\rm s}^0 = 0$; the Rabi frequencies of the probe, driving and pump fields at the entrance of the medium ($z = 0$) are $\Omega_{\rm pin} = 0.02\gamma_{31}$, $\Omega_{\rm cin} = 3.3\gamma_{31}$, and $\Omega_{\rm sin} = 2.0\gamma_{31}$, respectively. In addition, we always let $p_1 \equiv p_2 \equiv p$, because all parameters (except of ρ_{ij}, p, and z) are scaled by γ_{31}, so from now on, for simplicity we will omit γ_{31} when we give the parameter values in the following. To see more obviously the difference between the cases with and without the Doppler broadening, we first analyse the case without the Doppler broadening and then the case with the Doppler broadening.

3.1. Without Doppler broadening

Figure 2 illustrates population ρ_{ii} ($i = 1,2,3,4$), probe gain (absorption) ${\rm Im}\,\rho_{13}$, Rabi frequencies of the probe, driving and pump fields $\Omega_{\rm p}$, $\Omega_{\rm c}$, and $\Omega_{\rm s}$ versus propagation distance z (i.e. spatial evolution) for different values of p ($p_1 = p_2 = p$) without the Doppler broadening ($D = 0$).

It should be pointed out that according to the definitions of $\Omega_{\rm p}$, $\Omega_{\rm c}$, and $\Omega_{\rm s}$, we can say that: the spatial evolution rules, which will be given in the following discussion of this paper, of Rabi frequencies of the probe (i.e. LWI), driving and pump fields also are the spatial evolution rules of the intensities of the probe (i.e. LWI), driving and pump fields respectively.

Figures 2(a) and 2(b) show that: the variation rule of ρ_{ii} ($i = 1,2,3,4$) as functions of z when $p = 0$ is basically similar to that when $p = 1.0$. The inversionless condition $\rho_{33} - \rho_{11} < 0$ is always satisfied in the propagation processes of the probe, driving and pump fields; if ${\rm Im}\,\rho_{13} > 0$ is also simultaneously satisfied, we can obtain the gain without inversion, i.e. LWI gain (referred to gain in the following) and then LWI can be realized. In fact, the curves of ρ_{ii} ($i = 1,2,3,4$) versus z when $p = 0.2$ and $p = 0.7$ are also similar to that when $p = 1.0$. To reduce the length of this paper, the spatial evolution of ρ_{ii} ($i = 1,2,3,4$) for $p = 0.2$ and $p = 0.7$ are not given here.

From Fig. 2(c) we can see that: under the condition of $p = 0$ (i.e. SGC is absent), when the value of z is small ($z < 0.4$ cm), gain decreases monotonously with the increase of z; when the value of z is large enough ($z > 0.4$ cm), we only obtain absorption (${\rm Im}\,\rho_{13} < 0$). The size of gain and the length of propagation distance z in which gain exists (≈ 0.4 cm) are both very small. Under the condition of $p \neq 0$

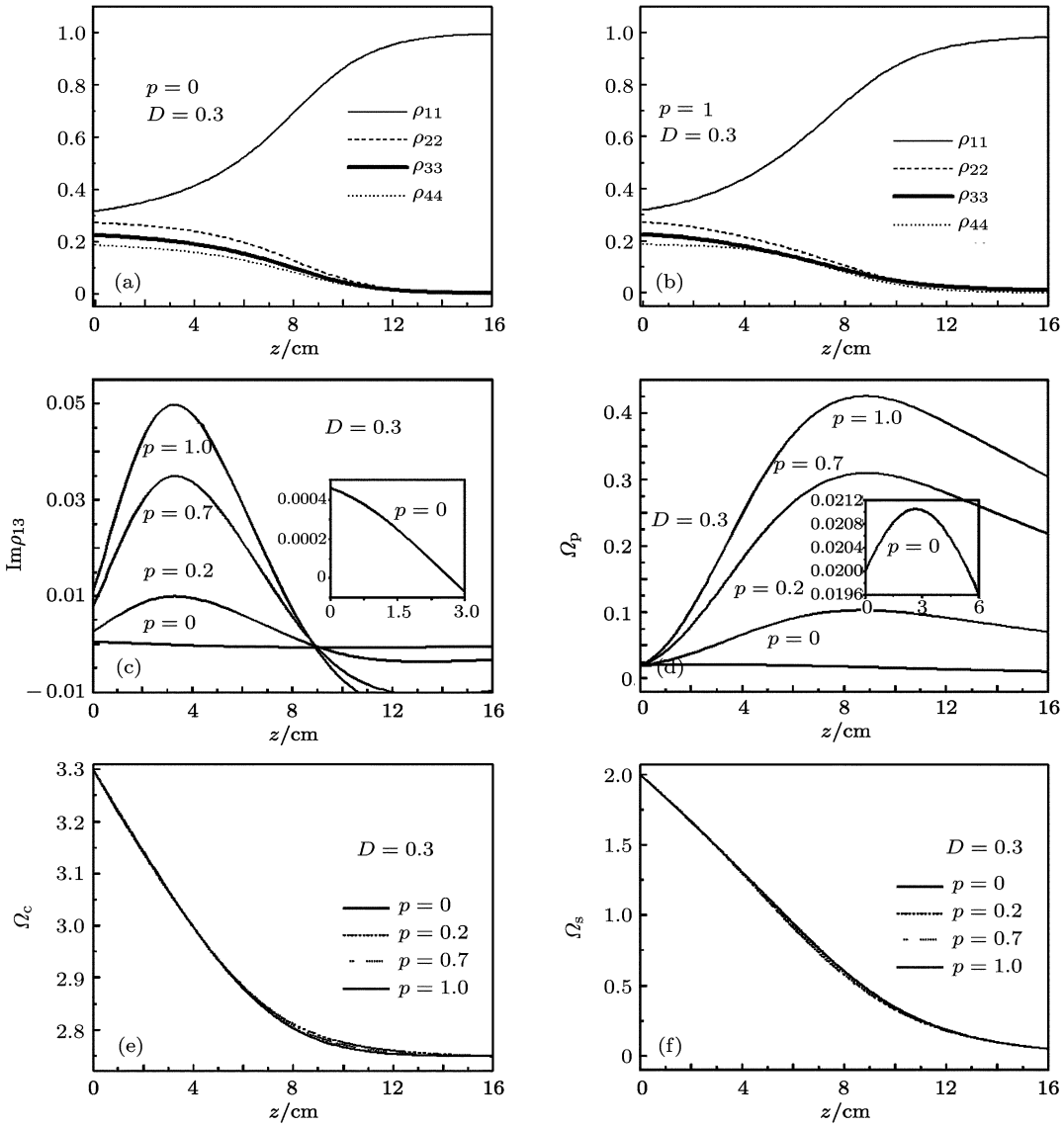


Fig. 2. ρ_{ii}, $\mathrm{Im}\,\rho_{13}$, Ω_p, Ω_c, and Ω_s as functions of z for different values of p ($p_1 = p_2 = p$). The parameter values are $\Omega_\mathrm{pin} = 0.02$, $\Omega_\mathrm{cin} = 3.3$, $\Omega_\mathrm{sin} = 2.0$, $\gamma_{31} = \gamma_{32} = 1$, $\gamma_{41} = \gamma_{42} = 1.2$, $\Delta_\mathrm{p}^0 = 4.9\gamma_{31}$, $\Delta_\mathrm{c}^0 = 0$, $\Delta_\mathrm{s}^0 = 0$, $D = 0$.

(i.e. SGC is present), when the value of z is small ($z < 5.0$ cm), $\mathrm{Im}\,\rho_{13}$ first increases and then decreases with the increase of z; When the value of z is large enough ($z > 5.0$ cm), we only obtain absorption. Changing the value of p does not change the variation rule of $\mathrm{Im}\,\rho_{13}$ with varying z. Regardless of the value of p, the system has the same range of propagation distance z (≈ 5.0 cm) in which gain occurs and the same value of z (≈ 2.3 cm) which corresponds to the gain maximum value $(\mathrm{Im}\,\rho_{13})_\mathrm{max}$. When the values of the other parameters keep unvarying, the value of gain decreases with the increase of p, the value of gain is the smallest when $p = 0$, the largest when $p = 1$; a much larger gain in the case with SGC than that in the case without SGC can be obtained. Figures 2(d) shows that: regardless of SGC being present or not, Ω_p first increases and then decreases with the increase of z; the maximum value of Ω_p, written as $(\Omega_\mathrm{p})_\mathrm{max}$, appears at the value of z which corresponds to $\mathrm{Im}\,\rho_{13} = 0$; with the continuous increase of z, the system only obtains absorption ($\mathrm{Im}\,\rho_{13} < 0$) and so Ω_p decreases monotonously. When $p = 0$, with the increase of z, Ω_p increases slowly in a short propagation distance (≈ 0.4 cm), then decreases apparently and then decreases to zero, When $p \neq 0$, with the increase of z, Ω_p increases rapidly in a long propagation distance (≈ 5.0 cm). For the same values of the other parameters, a much larger value of Ω_p in the case with SGC than that in the case without SGC can be obtained; the system for different values of p has roughly the same value of z which corresponds to $(\Omega_\mathrm{p})_\mathrm{max}$; $(\Omega_\mathrm{p})_\mathrm{max}$ increases with the increase of p, $(\Omega_\mathrm{p})_\mathrm{max}$ is

the largest when $p = 1$; this is because the value of gain is the largest when $p = 1$ (see Fig. 2(c)). Figures 2(e) and 2(f) show that: regardless of SGC being present or not, both Ω_c and Ω_s decrease monotonously with the increase of z before they reach a stable value, respectively; the basic reason is that the energy transfers gradually from the driving and pump fields to the probe field in the propagation processes of the probe, driving and pump fields. Relatively speaking, the influence of varying SGC strength (i.e. the value of p) on spatial evolution of Ω_c and Ω_s is not obvious.

In the above discussions, the values of the Rabi frequencies of the driving and pump fields at the entrance of the medium ($z = 0$) are $\Omega_{cin} = 3.3\gamma_{31}$ and $\Omega_{sin} = 2.0\gamma_{31}$, respectively. Varying the values of Ω_{cin} and Ω_{sin} will produce considerable influence on values and spatial evolution of $\mathrm{Im}\,\rho_{13}$ and Ω_p. To reduce the length of the paper, we only take the variation case of $\mathrm{Im}\,\rho_{13}$ at a special distance as an example to make a brief discussion.

Figure 3 denotes the probe gain (absorption) $\mathrm{Im}\,\rho_{13}$ as functions of Ω_{cin} and Ω_{sin} at $z = 1.0$ cm, figures 3(b) and 3(d) are enlargements of the curves corresponding to $p = 0$ in Figs. 3(a) and 3(c), respectively. It should be pointed out that in now and following discussions, corresponding populations always satisfy the inversionless condition $\rho_{33} - \rho_{11} < 0$, so we can obtain the gain without inversion, i.e. LWI gain if $\mathrm{Im}\,\rho_{13} > 0$, and from now on we no longer give out the spatial evolution of populations ρ_{ii} $(i = 1, 2, 3, 4)$.

It can be seen from Fig. 3 that: regardless of SGC being present or not, varying values of Ω_{cin} and Ω_{sin} have an obvious effect on the probe gain (absorption) $\mathrm{Im}\,\rho_{13}$; the gain maximum value can be obtained by choosing suitable (not more large) values of Ω_{cin} and Ω_{sin}. When $p \neq 0$ (i.e. SGC is present), for gain maximum values corresponding to different values of p, we obtain roughly the same value of Ω_{cin} (Ω_{sin}), and this value of Ω_{cin} (Ω_{sin}) is smaller than that corresponding to the gain maximum value in the case without SGC. From Fig. 3 we can also see that: the gain increases with the increase of p, in the case with SGC a much larger gain than that in the case without SGC can be obtained.

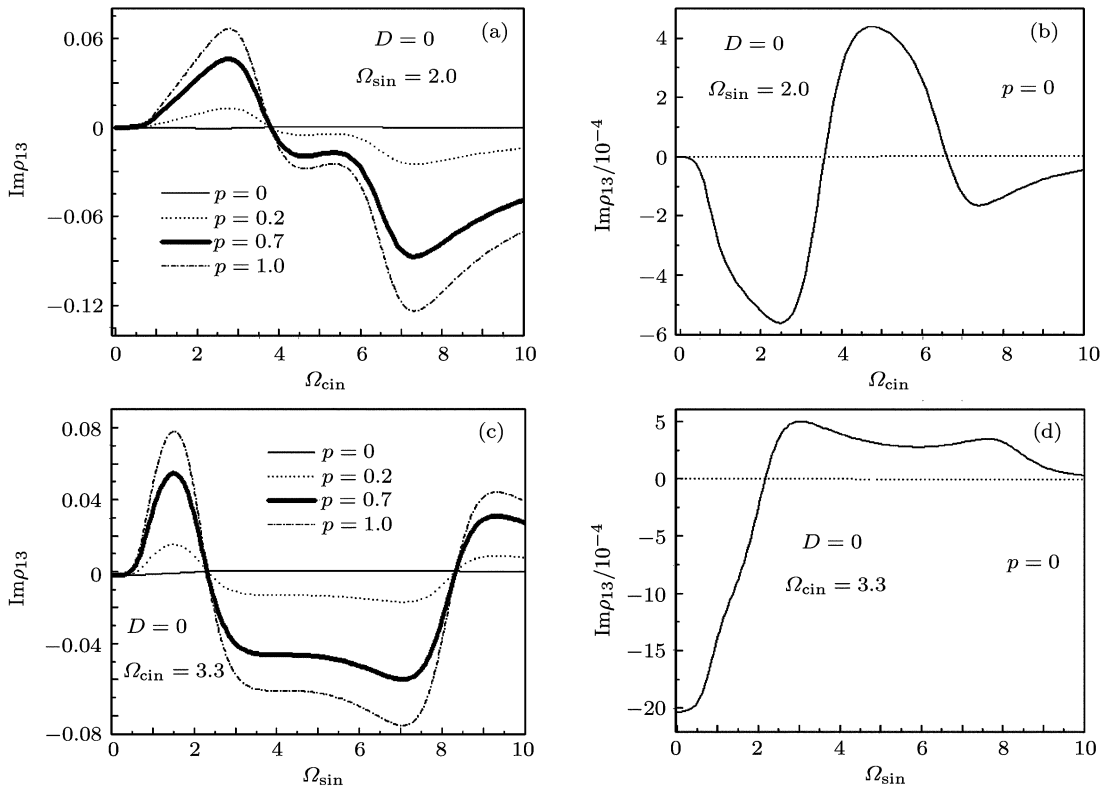


Fig. 3. $\mathrm{Im}\,\rho_{13}$ as functions of Ω_{cin} and Ω_{sin} at $z = 1.0$ cm, other parameters are the same as those used in Fig. 2.

3.2. With Doppler broadening

In the following we analyse the influence of SGC on the propagation effect in the quasi Λ-type four-level atomic system with Doppler broadening. The numerical calculation result shows that: when $D = 0$ (i.e., Doppler broadening is absent), varying propagation

directions of the probe and driving fields do not affect the variation rules of population ρ_{ii} $(i = 1, 2, 3, 4)$, probe gain (absorption) $\mathrm{Im}\,\rho_{13}$, Rabi frequencies of the probe, driving and pump fields Ω_p, Ω_c and Ω_s versus propagation distance z. Hence in the discussion of Subsection 3.1 we did not say that the propagation directions of the probe and driving fields are same or opposite. When $D \neq 0$ (i.e., the Doppler broadening is present), the variation rules of ρ_{ii} $(i = 1, 2, 3, 4)$, $\mathrm{Im}\,\rho_{13}$, Ω_p, Ω_c, and Ω_s as functions of z are very sensitive to variation of the propagation directions of the probe and driving fields. For the sake of clarity, we first analyse the co-propagating case and then the counter-propagating case.

3.2.1. The probe and driving fields are co-propagating

Figure 4 plots the probe gain (absorption) $\mathrm{Im}\,\rho_{13}$ and Rabi frequency of the probe field Ω_p as functions of propagation distance z (i.e. spatial evolution) for different values of p $(p_1 = p_2 = p)$ with $D = 0.3$, when the probe and driving fields are co-propagating. It should be pointed out that from now on we no longer give out spatial evolution of Rabi frequencies of the driving and pump fields Ω_c and Ω_s, due to the following two reasons: (i) the main goal of this paper is to study influences of the Doppler broadening, SGC and other system parameters on variation of LWI gain and intensity versus increasing propagation distance, i.e. propagation effect; (ii) our numerical result shows that in different cases both Ω_c and Ω_s always decrease monotonously with increasing z before they reach a stable value, respectively, although detailed situations of spatial evolution of Ω_c and Ω_s in different cases are different.

Comparing Figs. 4(a) and 4(b) with Figs. 2(c) and 2(d) we can obtain the following results. 1) For the same value of p, the variation rules of $\mathrm{Im}\,\rho_{13}$ and Ω_p as functions of z, when the Doppler broadening is present, are similar to those when the Doppler broadening is absent; however, when the Doppler broadening is present, the propagation distances in which gain exists, i.e., the propagation distances needed for reaching the maximum value of Ω_p becomes longer. 2) Similar to the case without the Doppler broadening, when the Doppler broadening is present, in the case without SGC ($p = 0$), the values of gain and Ω_p are very small; in the case with SGC ($p \neq 0$), the values of gain and Ω_p increase with increasing p, we can obtain the largest values of gain and Ω_p when $p = 1$.

From Figs. 5 and 6 we can obtain the following results. (I) Regardless of SGC being present or not, the propagation distance in which gain exists always increases monotonously with the increase of D, but the variation rule of the gain maximum value $(\mathrm{Im}\,\rho_{13})_\mathrm{max}$ with the increase of D in the case without SGC ($p = 0$) is much different from that in the case with SGC ($p = 1$. If $p = 0$ (Fig. 5(a)), $(\mathrm{Im}\,\rho_{13})_\mathrm{max}$ increases then decreases with the increase of D; when $D = 0.3$, we obtain the largest value of $(\mathrm{Im}\,\rho_{13})_\mathrm{max}$. Comparing Fig. 5(a) with Fig. 2(c), we know that: when $D < 0.8$, the value of $(\mathrm{Im}\,\rho_{13})_\mathrm{max}$ is larger than that $(\approx 1.25 \times 10^{-4})$ when $D = 0$; when $D = 0.8$, value of $(\mathrm{Im}\,\rho_{13})_\mathrm{max}$ is smaller than that $(\approx 1.25 \times 10^{-4})$ when $D = 0$. If $p = 1$ (Fig. 6(a)), $(\mathrm{Im}\,\rho_{13})_\mathrm{max}$ decreases with the increase of D monotonously, which is always smaller than that (≈ 0.072) when $D = 0$ (Fig. 2(c)). (II) By comparing Figs. 5(b) and 6(b) we can see that: the variation rule of the maximum value $(\Omega_\mathrm{p})_\mathrm{max}$ of Ω_p versus D when $p = 0$ is the same as that when $p = 1$.

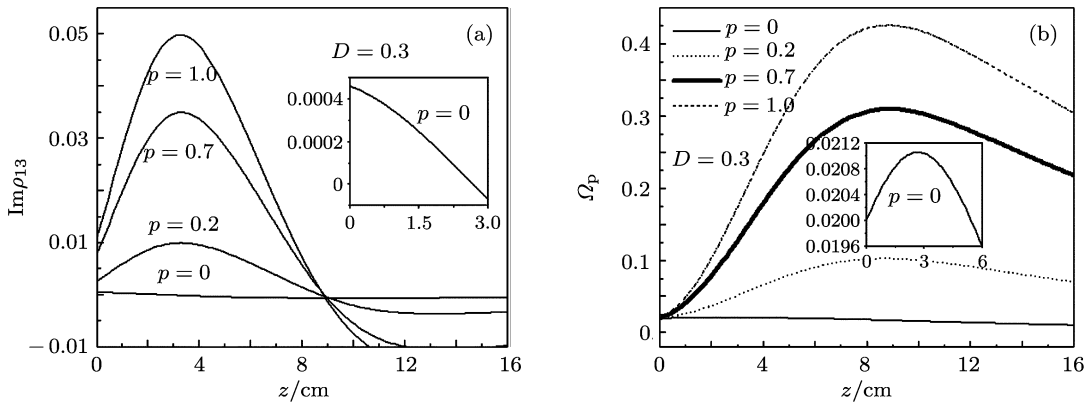


Fig. 4. $\mathrm{Im}\,\rho_{13}$ and Ω_p as functions of z for different values of p with $D = 0.3$ and other parameters are the same as those in Fig. 2 when the probe and driving fields are co-propagating.

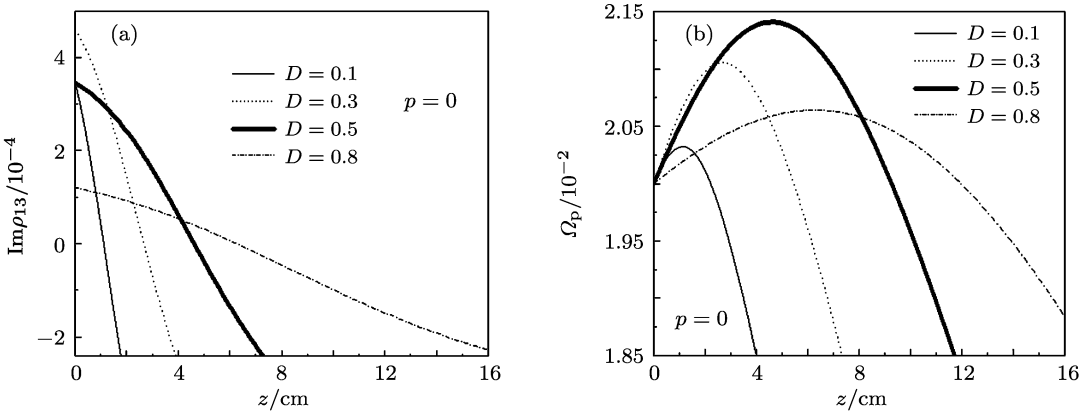


Fig. 5. $\mathrm{Im}\,\rho_{13}$ and Ω_p as functions of z for different values of D with $p = 0$ and other parameters are the same as those in Fig. 2 when the probe and driving fields are co-propagating.

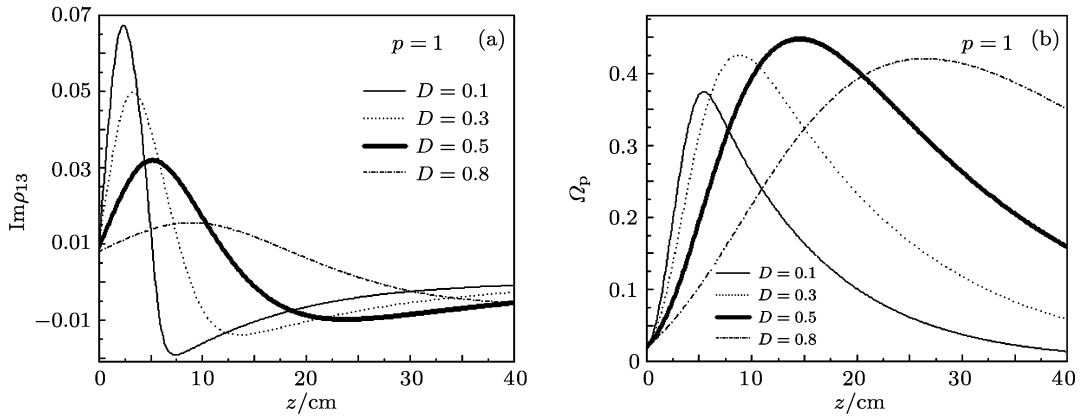


Fig. 6. $\mathrm{Im}\,\rho_{13}$ and Ω_p as functions of z for different values of D with $p = 1$ and other parameters are the same as those in Fig. 2 when the probe and driving fields are co-propagating.

The $(\Omega_\mathrm{p})_\mathrm{max}$ increases then decreases with the increase of D; when $D = 0.5$, we obtain the largest value of $(\Omega_\mathrm{p})_\mathrm{max}$, this also is the largest value of Ω_p, written as $(\Omega_\mathrm{p})_\mathrm{L}$. But in these two cases, the values of $(\Omega_\mathrm{p})_\mathrm{L}$ are different. When $p = 0$, $(\Omega_\mathrm{p})_\mathrm{L} \approx 0.021$ (Fig. 5(b)) and which is larger than that ($(\Omega_\mathrm{p})_\mathrm{L} \approx 0.020$) when $D = 0$ (Fig. 2(d)). When $p = 1$, $(\Omega_\mathrm{p})_\mathrm{L} \approx 0.45$ (Fig. 6(b)) and this is considerably larger than that ($(\Omega_\mathrm{p})_\mathrm{L} \approx 0.36$) when $D = 0$ (Fig. 2(d)). Very obviously, the value of D corresponding to $(\Omega_\mathrm{p})_\mathrm{L}$ is different from that corresponding to the largest value of $(\mathrm{Im}\,\rho_{13})_\mathrm{max}$, because $(\Omega_\mathrm{p})_\mathrm{L}$ depends on both the size of $(\mathrm{Im}\,\rho_{13})_\mathrm{max}$ and the length of propagation distance in which the gain exists.

Figure 7 illustrates $\mathrm{Im}\,\rho_{13}$ as a function of Ω_cin and Ω_sin at $z = 1.0$ cm for different values of D when $p = 0$ and $p = 1$, respectively. From Fig. 7 we can obtain the following results. i) Similar to the case without the Doppler broadening (Fig. 3), regardless of SGC being present or not, varying values of Ω_cin and Ω_sin has remarkable effect on the gain; the gain maximum value can be obtained by choosing suitable values of Ω_cin and Ω_sin; in the case with SGC ($p = 1$) a much larger gain than that in the case without SGC ($p = 0$) can be obtained. ii) The value of Ω_cin (Ω_sin) corresponding to the gain maximum value $(\mathrm{Im}\,\rho_{13})_\mathrm{max}$ varies with varying D. When $p = 0$ and the value of Ω_sin is kept fixed (see Fig. 7(a)), the value of Ω_cin corresponding to $(\mathrm{Im}\,\rho_{13})_\mathrm{max}$ decreases with the increase of D. When $p = 1$ and the value of Ω_sin is kept fixed (see Fig. 7(c)), the value of Ω_cin corresponding to $(\mathrm{Im}\,\rho_{13})_\mathrm{max}$ first decreases and then increases with the increase of D. When $p = 0$ and the value of Ω_cin is kept fixed (see Figs. 7(b)), the value of Ω_sin corresponding to $(\mathrm{Im}\,\rho_{13})_\mathrm{max}$ first decreases and then increases with the increase of D. When $p = 1$ and the value of Ω_cin is kept fixed (see Figs. 7(d)), the values of Ω_sin corresponding to $(\mathrm{Im}\,\rho_{13})_\mathrm{max}$ of different values of D are approximately the same.

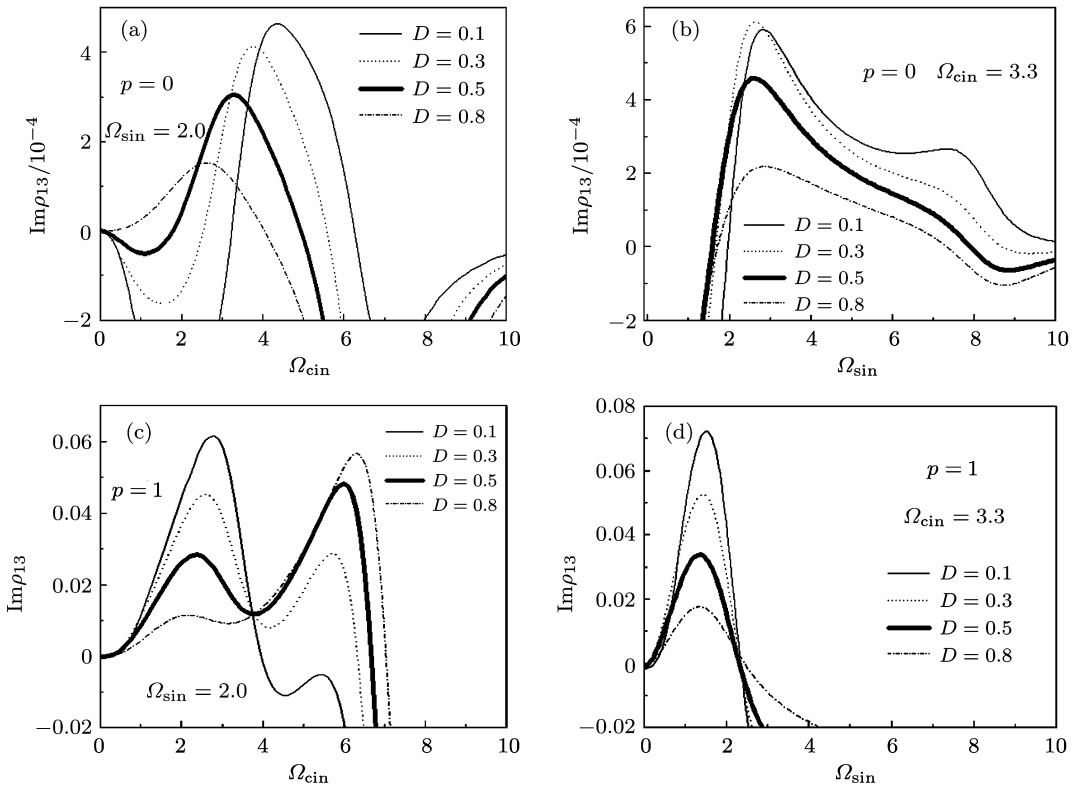


Fig. 7. $\mathrm{Im}\,\rho_{13}$ as a function of $\Omega_{\rm cin}$ and $\Omega_{\rm sin}$ at $z = 1.0$ cm, other parameters are the same as those in Fig. 2 when the probe and driving fields are co-propagating.

3.2.2. The probe and driving fields are counter-propagating

In the following we analyse the case of the counter-propagating probe and driving fields and compare it with the co-propagating case.

Figure 8 plots $\mathrm{Im}\,\rho_{13}$ and $\Omega_{\rm p}$ as functions of propagation distance z (i.e. spatial evolutions) for different values of p with $D = 0.3$ when the probe and driving fields are counter-propagating. Comparing Fig. 8 with Fig. 4 shows that: in the counter-propagating case we can obtain a conclusion similar to that in the co-propagating case. We do not repeat it again here but there is also an obvious difference between the two cases, i.e. the largest values of the gain and $\Omega_{\rm p}$ in the counter-propagating case are much smaller than those in the co-propagating case.

Figures 9 and 10 illustrate $\mathrm{Im}\,\rho_{13}$ and $\Omega_{\rm p}$ versus propagation distance z for different values of D when $p = 0$ and $p = 1$, respectively in the counter-propagating case. Comparing Fig. 9 (Fig. 10) with Fig. 5 (Fig. 6), we can obtain the following results. I) Similar to the co-propagating case, in the counter-propagating case, for a fixed value of D, the values of $(\Omega_{\rm p})_{\rm max}$ and $(\mathrm{Im}\,\rho_{13})_{\rm max}$ corresponding to $p = 1$ are much larger than those corresponding to $p = 0$. II) Different from the co-propagating case, in the counter-propagating case, regardless of SGC being present or not, the values of $(\Omega_{\rm p})_{\rm max}$ and $(\mathrm{Im}\,\rho_{13})_{\rm max}$ decrease monotonously with increasing D. III) Our numerical calculation result shows that: when $p = 0$ and the value of D is smaller ($D < 0.2$), for a fixed value of D, the values of $(\Omega_{\rm p})_{\rm max}$ and $(\mathrm{Im}\,\rho_{13})_{\rm max}$ in the counter-propagating case are larger than those in the co-propagating case; for example, when $D = 0.1$, the values of $(\Omega_{\rm p})_{\rm max}$ and $(\mathrm{Im}\,\rho_{13})_{\rm max}$ in the counter-propagating case are 5.138×10^{-4} and 0.02128 respectively; the values of $(\Omega_{\rm p})_{\rm max}$ and $(\mathrm{Im}\,\rho_{13})_{\rm max}$ in the co-propagating case are 3.267×10^{-4} and 0.02032 respectively. For other cases, i.e., when $p = 0$ and $D > 0.2$ or when $p = 1$ and D takes any value, for the same value of D, the values of $(\Omega_{\rm p})_{\rm max}$ and $(\mathrm{Im}\,\rho_{13})_{\rm max}$ in the counter-propagating case are always much smaller than those in the co-propagating case, even regardless of SGC being present or not, when $D \geq 0.5$ we only obtain absorption ($\mathrm{Im}\,\rho_{13} < 0$) in the counter-propagating case.

Figure 11 illustrates $\mathrm{Im}\,\rho_{13}$ as a function of $\Omega_{\rm cin}$ and $\Omega_{\rm sin}$ at $z = 1.0$ cm for $D = 0.1$ and $D = 0.3$, respectively when the probe and driving fields are counter-propagating. Here we do not give the spatial evolution of $D = 0.5$ and $D = 0.8$, which is given

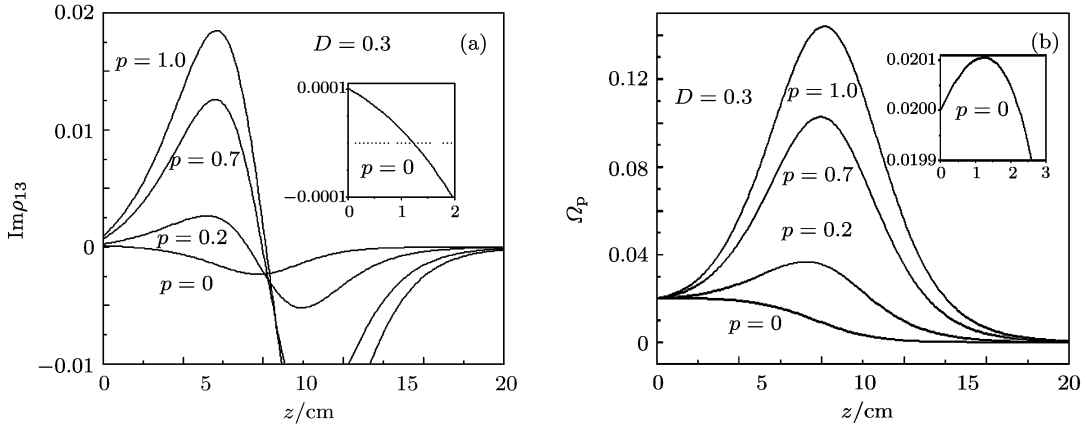


Fig. 8. $\mathrm{Im}\,\rho_{13}$ and Ω_{p} as functions of z for different values of p with $D = 0.3$ and other parameters are the same as those in Fig. 2 when the probe and driving fields are counter-propagating.

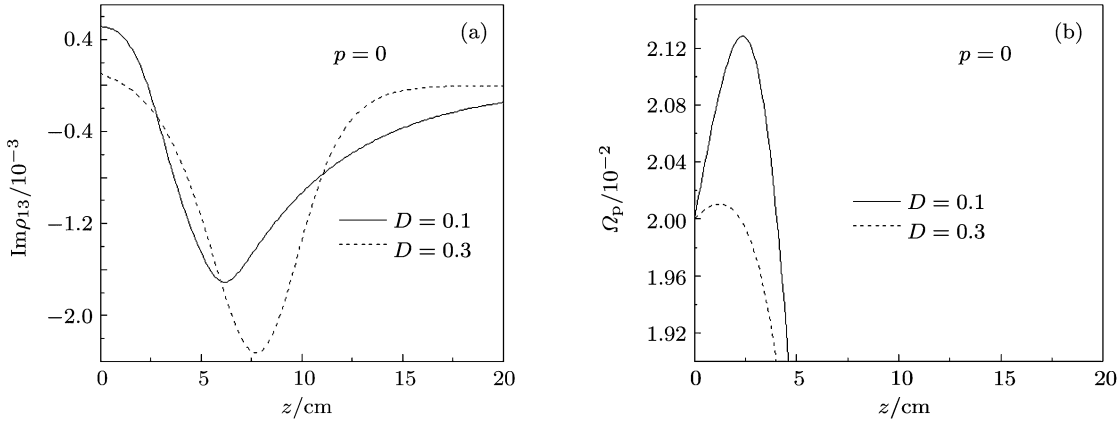


Fig. 9. $\mathrm{Im}\,\rho_{13}$ and Ω_{p} as functions of z for different values of D with $p = 0$ and other parameters are the same as those in Fig. 2 when the probe and driving fields are counter-propagating.

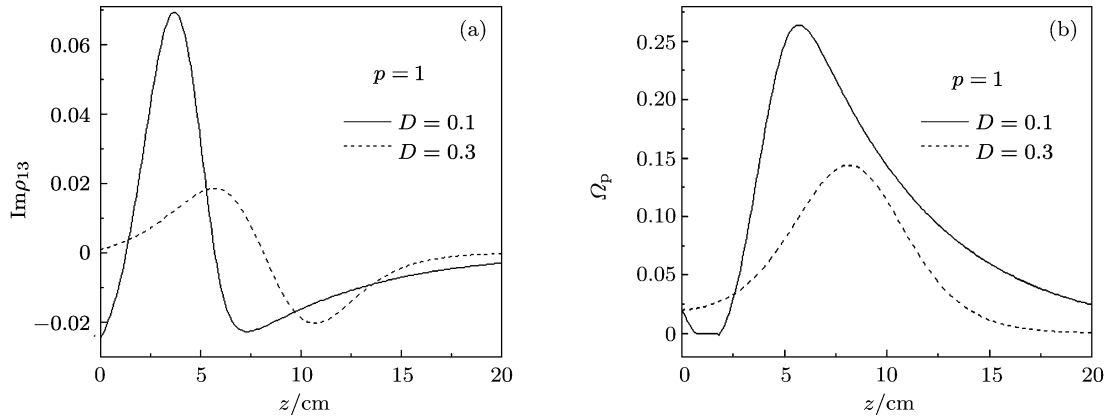


Fig. 10. $\mathrm{Im}\,\rho_{13}$ and Ω_{p} as functions of z for different values of D with $p = 1$ and other parameters are the same as those in Fig.2 when the probe and driving fields are counter-propagating.

in the co-propagating case (Fig. 7). This is because that regardless of Ω_{cin} and Ω_{sin} taking any values, we can only obtain absorption ($\mathrm{Im}\,\rho_{13} < 0$) in the counter-propagating case when $D \geq 0.5$ for $p = 0$ and $D > 0.3$ for $p = 1$. Comparing Fig. 7 with Fig. 11, we find that: the variation rule of the curves in the counter-propagating case (Fig. 11) is similar to that in the co-propagating case (Fig. 7). Regardless of SGC being present or not, varying values of Ω_{cin} and Ω_{sin} have an apparent effect on $\mathrm{Im}\,\rho_{13}$; the gain maximum value $(\mathrm{Im}\,\rho_{13})_{\mathrm{max}}$ can be obtained by choosing suitable values of Ω_{cin} and Ω_{sin}; a much larger gain in the case with SGC ($p = 1$) than that in the case without SGC ($p = 0$) can be obtained. Figure 11 also

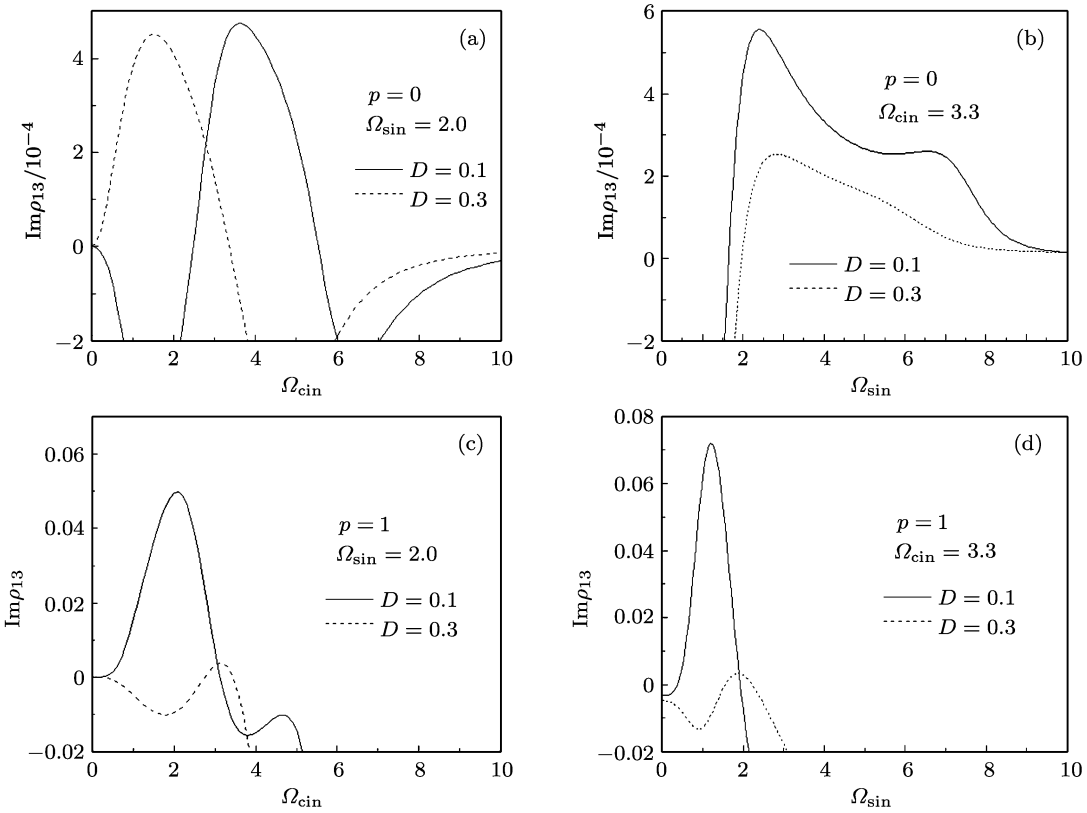


Fig. 11. $\rm Im\,\rho_{13}$ as a function of $\Omega_{\rm cin}$ and Ω_{sin} at $z = 1.0cm$, other parameters are the same as those used in Fig. 2 when the probe and driving fields are counter- propagating.

shows some considerable differences from the situation of the co-propagating case (Fig. 7): except the case of $p = 0$ and $\Omega_{\rm sin} = 2.0$, when other parameters are fixed and $D \geq 0.3$, for a fixed value of D, the values of $(\Omega_{\rm p})_{\rm max}$ and $(\rm Im\,\rho_{13})_{\rm max}$ in the counter-propagating case are obviously smaller than those in the co-propagating case.

In addition, our numerical calculation result shows that: regardless of SGC and Doppler broadening being present or not, propagation directions of the probe and driving fields being same or opposite, when other parameter values are kept fixed, the varying value of the probe detuning $\Delta_{\rm p}$ also has obvious effect on special evolutions of ρ_{ii} $(i = 1, 2, 3, 4)$, $\rm Im\,\rho_{13}$, $\Omega_{\rm p}$, $\Omega_{\rm c}$, and $\Omega_{\rm s}$. Larger values of gain and $\Omega_{\rm p}$ can be obtained by choosing suitable value of $\Delta_{\rm p}$. A detailed discussion of this problem is not discussed here in order to remain within the word count.

It should be pointed out again that according to the definitions of $\Omega_{\rm p}$, $\Omega_{\rm c}$, and $\Omega_{\rm s}$, we can say that: the spatial evolution rules of Rabi frequencies of the probe (i.e. LWI), driving and pump fields given above are the spatial evolution rules of the intensities of the probe (i.e. LWI), driving and pump fields.

4. Conclusions

In this paper we studied the influences of the Doppler broadening, spontaneously generated coherence (SGC) and other system parameters on propagation effect in a quasi Λ-type four-level atomic system. It is shown that: regardless of the Doppler broadening being present or not, when SGC is absent, with the increase of propagation distance, the gain of LWI, (i.e. the probe field) decreases monotonously but LWI intensity first increases and then decreases; when SGC is present, with the increase of propagation distance, both the LWI gain and intensity first increases and then decreases. When SGC is absent, the LWI gain maximum value first increases and then decreases with the increase of the Doppler broadening width D; when SGC is present, the LWI gain maximum value decreases monotonously with the increase of D. Regardless of the prescence of SGC, the length of propagation distance in which the LWI gain exists increases monotonously with the increase of D, when the propagation directions of the probe and driving fields are the same, but the situation is reversed when the propagation directions are opposite. The size of the LWI intensity is determined by both the size of the LWI gain and the length of propagation distance in which

the LWI gain exists. The value of D which corresponds to the largest LWI gain is different from that corresponding to the largest LWI intensity. When the Doppler broadening is present, the much larger LWI gain and intensity than those without the Doppler broadening can be obtained by choosing appropriate values of D and SGC strength. Generally speaking, regardless of SGC being present or not, the values of the LWI gain and intensity in the co-propagating case are much larger than those in the counter-propagating case. However, when SGC is absent and the value of D is smaller, the values of the LWI gain and intensity in the counter-propagating case are larger than those in the co-propagating case. The LWI gain and intensity increase with the increase of SGC strength; when SGC is present, much larger LWI gain and intensity than those in the case without SGC can be obtained. Variations of the values of the probe detuning ($\Delta_{\rm p}$), the Rabi frequencies of the driving and pump fields at the entrance of the medium ($\Omega_{\rm cin}$ and $\Omega_{\rm sin}$), also have considerable effect on spatial evolutions of the LWI gain and intensity, choosing appropriate values of $\Delta_{\rm p}$, $\Omega_{\rm cin}$, and $\Omega_{\rm sin}$ can remarkably enhance the LWI gain and intensity.

References

[1] Zhou P and Swain S 1996 *Phys. Rev. Lett.* **77** 3995

[2] Zhou P and Swain S 1997 *Phys. Rev. lett.* **78** 832

[3] Gong S Q, Paspalakis E and Knight P L 1998 *J. Mod. Opt.* **45** 2433

[4] Menon S and Agarwal G S 1999 *Phys. Rev.* A **61** 013807

[5] Ghafoor F, Zhu S Y and Zubairy M S 2000 *Phys. Rev.* A **62** 013811

[6] Wu J H and Gao J Y 2002 *Phys. Rev.* A **65** 063807

[7] Ma H M, Gong S Q, Liu C P, Sun Z R and Xu Z Z 2003 *Opt. Commun.* **223** 97

[8] Hou B P, Wang S J, Yu W L and Sun W L 2004 *Phys. Rev.* A **69** 053805

[9] Li J H, Yang W X and Peng J C 2004 *Chin. Opt. Lett.* **2** 302

[10] Liu C P, Gong S Q, Fan X J and Xu Z Z 2004 *Opt. Commun.* **239** 383

[11] Berman P R 2005 *Phys. Rev.* A **72** 035801

[12] Gonzalo I, Antón M A, Carreño F and Calderón O G 2005 *Phys. Rev.* A **72** 033809

[13] Niu Y P and Gong S Q 2006 *Phys. Rev.* A **73** 053811

[14] Bai Y F, Guo H, Han D A and Sun H 2005 *J. Opt.* B **7** 35

[15] Li J H, Chen A X, Liu J B and Xie X T 2006 *Chin. Phys.* **15** 721

[16] Ma H M, Gong S Q, Sun Z R, Li R X and Xu Z Z 2006 *Chin. Phys.* **15** 2588

[17] Chen J, Liu Z D, Zheng J and Fang H J 2007 *Acta Phys. Sin.* **56** 6441 (in Chinese)

[18] Ma H, Tan X, Tian S F, Tong D M and Fan X J 2007 *Chin. Phys.* **16** 2400

[19] Sahrai M 2008 *Eur. Phys. J. Special Topics* **160** 383

[20] Li A J, Song X L, Wei X G, Wang L and Gao J Y 2008 *Phys. Rev.* A **77** 053806

[21] Das S and Agarwal G S 2008 *Phys. Rev.* A **77** 033850

[22] Yan X A, Song J P, Yin B Y, Jiang W J, Zheng H B and Zhang Y P 2008 *Acta Phys. Sin.* **57** 3538 (in Chinese)

[23] Yang X H and Zhu S Y 2008 *Phys. Rev.* A **77** 063806

[24] Yang Y L, Wang L, Liu Z B, Lu H W and Fan X J 2009 *Acta Phys. Sin.* **58** 3161 (in Chinese)

[25] Osman K I, Hassan S S and Joshi A 2009 *Eur. Phys. J.* D **54** 119

[26] For a review paper for LWI see Mompart J and Corbalán R 2000 *J. Opt.* B: *Quantum and Semiclas. Opt.* **2** R7

[27] For a review article for EIT see Marangos J P 1998 *J. Mod. Opt.* **45** 471

[28] Lü C H, Tan L and Tan W T 2011 *Acta Phys. Sin.* **60** 024204 (in Chinese)

[29] Yang B D, Gao J, Liang Q B, Wang J, Zhang T C and Wang J M 2011 *Chin. Phys.* B **20** 044202

[30] For a review article for CPT see. Arimondo E 1996 in *Progress in Optics* XXXV, ed. Wolf E (Amsterdam: North-Holland) p. 257

[31] Scully O M 1991 *Phys. Rev. Lett.* **67** 1855

[32] Waldmueller I, Wanke M C and Chow W W 2007 *Phys. Rev. Lett.* **99** 117401

[33] Kilin S Y, Kapale K T and Scully M O 2008 *Phys. Rev. Lett.* **100** 173601

[34] Liberato S D and Ciuti C 2009 *Phys. Rev. Lett.* **102** 136403

[35] Scully M O 2010 *Phys. Rev. Lett.* **104** 207701

[36] Bennett C H and Divincenzo D P 2000 *Nature* **404** 247

[37] Vemuri G and Agarwal G S 1996 *Phys. Rev.* A **53** 1060

[38] Mompart J, Peters C and Corbalán R 1998 *Phys. Rev.* A **57** 2163

[39] Boon J R, Zekou E, McGloin D and Dunn M H 1998 *Phys. Rev.* A **58** 2560

[40] Ahufinger V, Mompart J and Corbalán R 1999 *Phys. Rev.* A **60** 614

[41] Fan X J, Xu H, Tian S F, Tong D M and Xu Z Z 2004 *Opt. Commun.* **241** 399

[42] Xu W H and Gao J Y 2005 *Chin. Phys.* **14** 2496

[43] Lukin M D, Scully M O and Welch G R 1996 *Laser Phys.* **6** 436

[44] Yelin S F, Lukin M D, Scully M O and Mandel P 1998 *Phys. Rev.* A **57** 3858

[45] Mompart J, Ahufinger V, Corbalán R and Parti F 2000 *J. Opt.* B: *Quantum and Semiclass. Opt.* **2** 359

[46] Qiao H X, Yang Y L, Tan X, Tong D M and Fan X J 2008 *Chin. Phys.* B **17** 3734